

Zero-field composite Fermi liquid in twisted semiconductor bilayers

Hart Goldman*, Aidan P. Reddy*, Nisarga Paul*, and Liang Fu

Department of Physics, Massachusetts Institute of Technology, Cambridge, MA 02139

(Dated: October 25, 2023)

Recent experiments have produced evidence for fractional quantum anomalous Hall (FQAH) states at zero magnetic field in the semiconductor moiré superlattice system $t\text{MoTe}_2$. Here we argue that a composite fermion description, already a unifying framework for the phenomenology of 2d electron gases at high magnetic fields, provides a similarly powerful perspective in this new context. To this end, we present exact diagonalization evidence for composite Fermi liquid states at zero magnetic field in $t\text{MoTe}_2$ at fillings $n = \frac{1}{2}$ and $n = \frac{3}{4}$. We dub these non-Fermi liquid metals anomalous composite Fermi liquids (ACFLs), and we argue that they play a central organizing role in the FQAH phase diagram. We proceed to develop a long wavelength theory for this ACFL state that offers concrete experimental predictions upon doping the composite Fermi sea, including a Jain sequence of FQAH states and a new type of commensurability oscillations originating from the superlattice potential intrinsic to the system.

Introduction. Recently, signatures of fractional quantum anomalous Hall (FQAH) states at zero magnetic field have been observed by optical measurements on twisted bilayer MoTe_2 ($t\text{MoTe}_2$) at fractional fillings of the moiré unit cell $n = \frac{2}{3}$ and $\frac{3}{5}$ [1]. In a separate work, the charge gap of the putative FQAH state at $n = \frac{2}{3}$ was measured [2]. FQAH states in twisted homobilayers of transition metal dichalcogenides (TMD) were theoretically predicted as a consequence of topological moiré bands [3], spontaneous ferromagnetism, and strong correlations [4–7]. These recent observations provide new motivation to explore the phenomenology and phase diagram of partially filled Chern bands in $t\text{MoTe}_2$ and beyond [8, 9].

Unlike Landau levels, Chern band systems can exhibit competition between incompressible FQAH states [10–18] and more conventional broken symmetry phases enabled by the presence of a periodic lattice structure, such as charge ordered phases [19–21] and generalized Wigner crystals [22–25], or conducting phases [26–28] like Fermi liquids and even superconductors. Exotic quantum critical phases have also been shown to appear in half-filled flat Chern bands [29]. As a result, the global phase diagram of partially filled Chern bands is potentially much richer than that of Landau levels, calling for systematic study.

In this work, we focus on the physics of twisted TMD bilayers at even-denominator filling factors, which have not yet received attention. We present numerical evidence from continuum model exact diagonalization (ED) calculations of gapless metallic states at filling factors $n = \frac{1}{2}$ and $\frac{3}{4}$. Remarkably, depending on the twist angle, two types of ferromagnetic metals with full spin/valley polarization are found. At larger twist angle, the ground state is a Fermi liquid. In contrast, at smaller twist angles where strong interaction effect induces odd-denominator FQAH states, we find non-Fermi liquid metals of composite fermions at $n = \frac{1}{2}$ and $\frac{3}{4}$. These states share features with the composite Fermi liquid (CFL) at

high magnetic fields [30, 31], but are “enriched” by the underlying moiré superlattice. We dub these zero-field non-Fermi liquid states “anomalous composite Fermi liquids” (ACFLs).

Synonymously with the CFL phases in Landau level systems, we propose the ACFL as the parent state of the FQAH phase diagram at $B = 0$ [32–34]. Indeed, based on our ED study, we argue that the prominent FQAH states at $n = \frac{2}{3}$ and $\frac{3}{5}$ in twisted TMD homobilayers are descendants of the ACFL state at $n = \frac{1}{2}$. These states fall along a Jain sequence of FQAH states, which we show emerges by doping the ACFL.

We further reveal the unique phenomenology of the ACFL state itself. Perhaps most strikingly, the ACFL resistivity and thermodynamic properties experience *intrinsic commensurability oscillations* as a function of density, ρ_e , at $B = 0$. This behavior contrasts both with an ordinary Fermi liquid and a CFL in a Landau level [35–45]. Close to the ACFL state, we find the oscillations are periodic in $1/\delta\rho_e$ and occur at large integers j satisfying

$$\frac{1}{\delta\rho_e} \propto \frac{j + \phi}{k_F Q}, \quad (1)$$

where $\delta\rho_e \equiv \rho_e - \bar{\rho}$ is the doping density from half filling, Q is the moiré superlattice wave vector, $k_F = \sqrt{4\pi\bar{\rho}}$ is the composite Fermi wave vector, and ϕ is a phase shift. For the ACFL state at a particular even-denominator filling fraction such as $\bar{n} = \frac{1}{2}$, k_F is proportional to Q , meaning that the doping density, $\delta\rho_e$, associated with the commensurability oscillation is inversely proportional to the moiré unit cell area. As a result, the corresponding filling fraction, $n = \bar{n} + \delta n$, is universal.

Eq. (1) is both a consequence of the attachment of flux to charge in the ACFL – which causes the composite fermions to feel an effective magnetic field upon doping – and the system’s intrinsic moiré potential. In contrast, commensurability oscillations in CFLs in Landau level systems require an *externally supplied* periodic potential. In addition to commensurability oscillations, a distinguishing feature of a CFL (at zero or finite field) is a large DC Hall angle, $\theta_H = \arctan(\sigma_{xy}/\sigma_{xx})$, which approaches $\pi/2$ in the clean limit [30].

* These authors contributed equally to the development of this work

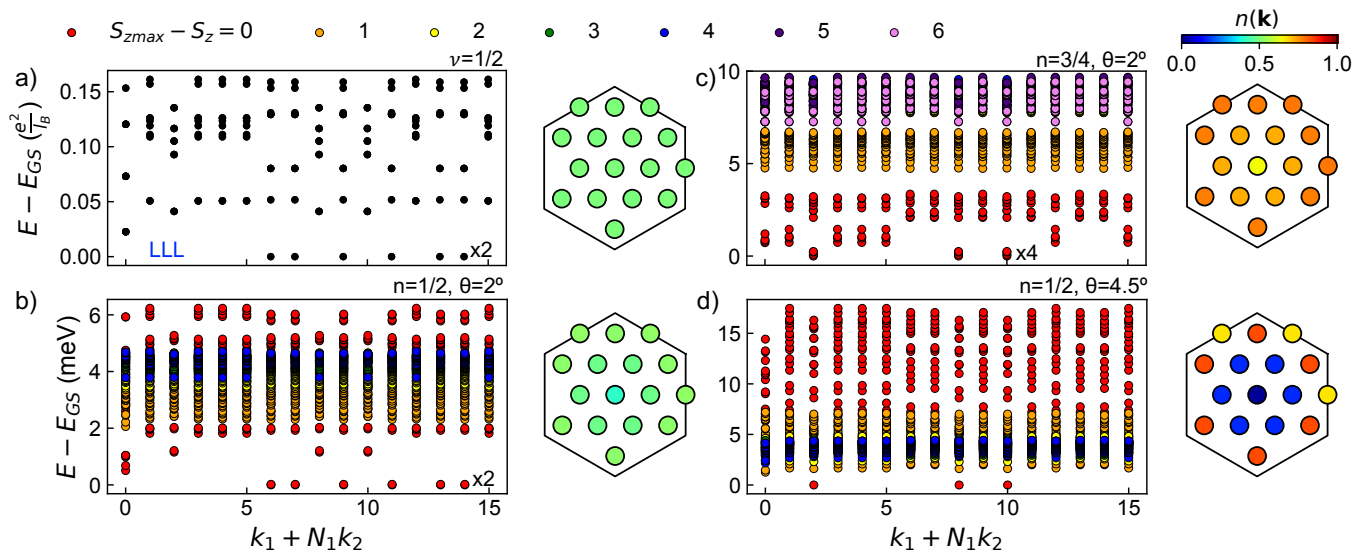


FIG. 1. **Zero-field and ferromagnetic Fermi liquid in semiconductor moiré bands.** Low-lying spectrum as a function of many-body crystal momentum (see the Supplemental Material for elaboration) of the (a) half-filled LLL and (b) lowest moiré band at a twist angle $\theta = 2^\circ$ with a Coulomb interaction. Occupation numbers of the Bloch states averaged over the degenerate ground state manifolds (see main text), $n(\mathbf{k}) \equiv \sum_{i \in GS} \langle \Psi_i | c_{\mathbf{k}}^\dagger c_{\mathbf{k}} | \Psi_i \rangle / N_{GS}$, are also shown. Full spin polarization is assumed in the LLL whereas all possible S_z sectors are considered in the moiré band. Analogous data at (c) $\theta = 2^\circ$, $n = \frac{3}{4}$ and (d) $\theta = 4.5^\circ$, $n = \frac{1}{2}$. In each case the lowest 20 energy levels within each (\mathbf{k}, S_z) sector are shown. In (b-d) a dielectric constant $\epsilon = 10$ is used.

CFL phases are expected to exhibit non-Fermi liquid observable features, some of which may be accessible as new platforms are developed realizing the ACFL. For example, the thermodynamic entropy of the ACFL state can be measured from the change in chemical potential with temperature through a Maxwell relation [46, 47]. In the clean limit, because gauge fluctuations lead to a logarithmic mass enhancement of composite fermions, the entropy of ACFL state should also be enhanced [48], $s(T)/T \sim m_*(T) \sim \log T$ [30], compared to the linear temperature dependence of an ordinary Fermi liquid, $s(T)/T \sim \text{constant}$. In systems where the electronic Coulomb interaction is screened by a nearby metallic gate, this enhancement becomes a power law, $s(T)/T \sim T^{-1/3}$.

Motivation. In ordinary Landau level quantum Hall systems, the existence of a CFL phase can be understood through flux attachment. At even-denominator filling $\nu = 2\pi\rho_e/B = \frac{1}{2q}$, where q is an integer, ρ_e is the electron density, and B is the external magnetic field, attaching $2q$ flux quanta to each electron completely screens the magnetic field, leading to an effective system of composite fermions in effective magnetic field $b_* = B - 2q(2\pi\rho_e) = 0$. As a result, the composite fermions form a Fermi surface strongly coupled to an emergent gauge field [30]. Upon doping away from $\nu = \frac{1}{2q}$, the composite fermions feel a nonvanishing magnetic field and fill Landau levels, leading to the Jain sequence of observed fractional quantum Hall phases,

$$\nu_{\text{Jain}} = \frac{p}{2qp - 1}, \quad (2)$$

where p is the number of filled composite fermion Landau levels [32, 33].

A similar picture should be applicable to twisted TMD bilayers in the absence of a physical magnetic field, when (1) interactions spontaneously drive all carriers into the Chern band of one valley; (2) the Coulomb Hamiltonian projected to the Chern band sufficiently resembles that of the lowest Landau level (LLL); and (3) the band dispersion is small relative to the system's characteristic interaction energy scale $\sim e^2/(\epsilon a_M)$. When these conditions are satisfied, the problem can be approximately mapped to that of a partially filled Landau level. One might therefore expect that any of the quantum Hall phases in a Landau level at filling ν should be possible in a flat $C = 1$ band at the same filling. The challenge is to find situations in which such physics succeeds over other phases that are not possible in Landau levels. Hence, once a material is known to exhibit the FQAH effect, it is natural to anticipate that other essential features of the fractional quantum Hall phase diagram also occur in the same material, such as the convergence of Jain sequence FQAH phases into a metallic CFL at half-filling.

Numerical evidence for ACFL. We now provide numerical evidence for the ACFL in $t\text{MoTe}_2$. The nontrivial layer pseudospin structure of this system's Bloch wavefunctions endows its moiré bands with topological character [3]. In particular, the first moiré valence band in each valley has $|C| = 1$, with opposite signs in opposite valleys due to time-reversal symmetry. We study the continuum model of $t\text{MoTe}_2$ with Coulomb interaction $U(r) = \frac{e^2}{\epsilon r}$ projected to the lowest moiré band, using finite size ED with torus geometry [8]. Further

details of the model and methodology are provided in the Supplemental Material.

To establish a benchmark for a CFL on a finite-size torus, we show the low-lying many-body spectrum of the half-filled LLL on a torus with 16 flux quanta in Fig. 1(a). Given our system geometry, the spectrum features 12 exactly degenerate ground states with 2 in each of 6 momentum sectors. The momentum quantum numbers of the degenerate ground states reflect the most compact possible composite Fermi sea configurations [14]. There are 6 such configurations – one composite fermion is accounted for by occupying the state at the center of the Brillouin zone, 6 more by occupying the set of closest points, and the final one by occupying any one of the 6 next closest points. The additional factor of 2 in the overall ground state degeneracy is enforced by the non-commuting center-of-mass magnetic translations [49]. We also show the momentum space occupation numbers of electron Bloch states averaged over the ground state manifold. The Bloch state occupation is uniform despite the presence of a composite Fermi sea.

Next, in Fig. 1(b), we show the many-body spectrum of the $\theta = 2^\circ$ lowest $t\text{MoTe}_2$ band at filling $n = \frac{1}{2}$ on the corresponding 16-unit-cell torus across all possible $S_z \geq 0$ sectors. First, we observe that the lowest-lying states have $S_z = S_{z,\text{max}} = 4$, indicating spontaneous, full spin/valley polarization. Moreover, these states have the same momentum quantum numbers as their partners in the LLL, providing evidence for a composite Fermi sea. The momentum space occupation numbers are nearly uniform as in the LLL, demonstrating that the system is *not* a ferromagnetic Fermi liquid. In Fig. 1(c), we show an ED spectrum at $n = \frac{3}{4}$ that exhibits full valley polarization and similarly resembles its partner in the LLL, which is shown in the Supplemental Material.

In Fig. 1(d), we contrast these findings with $n = \frac{1}{2}$ at a larger twist angle $\theta = 4.5^\circ$. Here, the lowest-energy states are still fully spin/valley polarized, but their many-body momenta are those expected from simply occupying the moiré band Bloch states with lowest energy, indicating a Fermi liquid phase. Moreover, the Bloch state occupation numbers in Fig. 1(c) exhibit a sharp drop across the Fermi surface expected for non-interacting, spin-polarized holes.

Effective theory of the ACFL. With this motivation, we propose a long wavelength effective theory of the ACFL in a Chern band at half-filling, $n = \frac{1}{2}$,

$$\begin{aligned} \mathcal{L}_{\text{ACFL}} = & \psi^\dagger \left[i\partial_t + a_t + A_t + \mathcal{V}(\mathbf{x}) \right] \psi \\ & - \frac{1}{2m_*} |(i\partial_i + a_i + A_i)\psi|^2 - V(\rho_e) \\ & - \frac{1}{2} \frac{1}{4\pi} \varepsilon_{\mu\nu\lambda} a_\mu \partial_\nu a_\lambda - a_t \bar{\rho}. \end{aligned} \quad (3)$$

Here ψ is the composite fermion field, m_* is an effective mass; $V(\rho_e)$ is the density-density interaction potential; $a_\mu = (a_t, a_x, a_y)$ is a fluctuating Chern-Simons statistical gauge field; and $A_\mu = (A_t, A_x, A_y)$ is the background

electromagnetic gauge field. We denote the value of the charge density at half filling by $\bar{\rho}$, such that the charge per unit cell is $\bar{n} \equiv \bar{\rho} \times (\text{unit cell area}) = \frac{1}{2}$. Importantly, although we focus on $n = \frac{1}{2}$ here, the theory for the ACFL at $n = \frac{3}{4}$ is easily obtained by attaching 4 flux quanta and acting with a particle-hole transformation (subtracting a filled $C = 1$ band). We expect its universal properties to be essentially the same as the ACFL at $n = \frac{1}{2}$. In the Supplemental Material, we discuss how Eq. (3) can be constructed from a parton mean field construction along similar lines to Ref. [27], which also considered ACFL type phases in flat Chern bands (we note here that the Supplemental Material also includes the additional Refs. [50–66]).

The theory in Eq. (3) closely resembles the Halperin-Lee-Read (HLR) theory of half-filled Landau levels [30]. This is not surprising: the $|C| = 1$ Chern band in twisted TMD bilayers can be thought of as carrying an emergent magnetic flux of one flux quantum per unit cell, which arises from the skrymion lattice configuration of “Zeeman” field acting on the layer pseudospin [3]. Nevertheless, there are two major differences with the standard HLR theory for a half-filled Landau level. The first is the final term, which alters the usual flux attachment constraint. Using the equation of motion for a_t ,

$$\rho_e = \bar{\rho} + \frac{1}{2} \frac{1}{2\pi} (\nabla \times \mathbf{a}), \quad (4)$$

where we have used the fact that the physical electron density coincides with that of the composite fermions, $\rho_e = \delta\mathcal{L}_{\text{ACFL}}/\delta A_t = \psi^\dagger\psi$, and boldface denotes spatial vectors. At half-filling of the Chern band, $n = \bar{n} = \frac{1}{2}$, meaning that by Eq. (4) the gauge flux per unit cell must vanish, and the composite fermions form a Fermi surface (as above, we use n to denote charge per unit cell).

The second difference is that Eq. (3) *includes the effect of the moiré superlattice*, in the form of a periodic scalar potential,

$$\mathcal{V}(\mathbf{x}) = \mathcal{V}_0 \sum_{n=1}^3 \cos(\mathbf{Q}_n \cdot \mathbf{x}), \quad (5)$$

where \mathbf{Q}_n are the moiré superlattice wave vectors (see Supplemental Material). The full scalar potential felt by the composite fermions is therefore $\mathcal{V}(\mathbf{x}) + A_t$, where A_t includes any additional probe fields. We will see that the presence of this term leads to commensurability oscillations which are unique to the ACFL.

Although the theory in Eq. (3) should correctly reproduce long wavelength, universal observable properties, we emphasize that this theory is not meant to completely incorporate microscopic details. For example, it does not give the correct algebra of density operators, nor does it incorporate the composite fermion dipole moment. Rather, we expect that should a complete, band-projected theory be constructed, then Eq. (3) could be understood as its long wavelength limit. For recent efforts to develop band-projected composite fermion theories

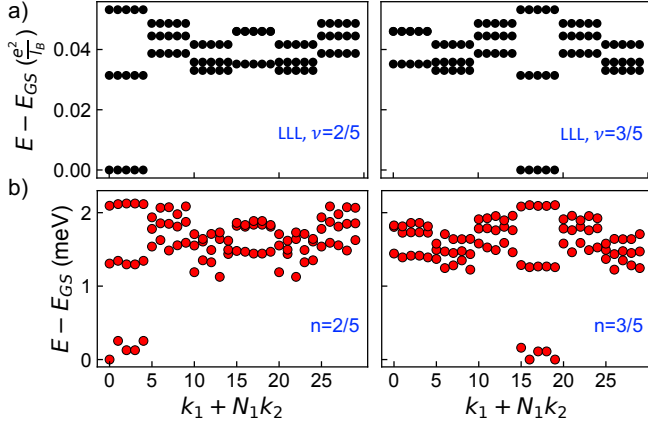


FIG. 2. **Joint sequence states at $n = \frac{2}{5}, \frac{3}{5}$.** (a) Low-lying spectrum of the LLL with Coulomb interaction on a torus with 30 flux quanta at $\nu = \frac{2}{5}$ and $\frac{3}{5}$. (b) Corresponding data for the lowest moiré band at $\theta = 2^\circ$, $\epsilon = 10$. The moiré ground state manifold has the same momentum quantum numbers and approximate fivefold topological ground state degeneracy as the LLL. In each case the lowest 3 fully spin polarized states in each momentum sector are shown.

in the context of the LLL, see Refs. [67–70].

FQAH sequence. Doping away from half-filling by tuning charge density or applied magnetic field causes the composite fermions to feel a net magnetic field and fill Landau levels. As a result, we can immediately predict a Jain sequence of FQAH states in $t\text{MoTe}_2$ corresponding to integer quantum Hall states of composite fermions. Like fractional Chern insulator states developed earlier [16–18, 71, 72], these FQAH phases are topological orders enriched with (super)lattice symmetry. Say that the composite fermions fill p Landau levels,

$$\nu_\psi = 2\pi \frac{\langle \psi^\dagger \psi \rangle}{b_*} = p, \quad b_* = \nabla \times (\mathbf{a} + \mathbf{A}), \quad (6)$$

where b_* is the total magnetic field felt by the composite fermions. Combining the flux attachment constraint, Eq. (4), with Eq. (6), we can relate the electron density to the applied magnetic field, $B = \nabla \times \mathbf{A}$,

$$\rho_e(B) = \frac{p}{2p-1} \left(2\bar{\rho} - \frac{B}{2\pi} \right). \quad (7)$$

The Streda formula then implies that one will measure Landau fans extending to $B = 0$, with slopes that fall on the Jain sequence (see Fig. 3),

$$\frac{d\rho_e}{dB} = \sigma_{xy} = -\frac{p}{2p-1}. \quad (8)$$

For the FQAH sequence proximate to $n = \frac{3}{4}$, one obtains FQAH states on the sequence, $n = 1 - \frac{p}{4p-1}$.

It is instructive to multiply Eq. (7) on both sides by the su-

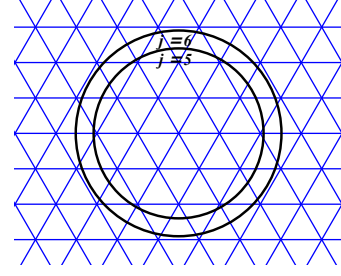


FIG. 3. **Commensurability oscillations.** Schematic of cyclotron orbits at special commensurate values. For $j \geq 5$, $\frac{1}{2} < \rho_e < \frac{3}{5}$.

perlattice unit cell area to obtain the simple expression,

$$n = \frac{p}{2p-1} (1 - n_\Phi), \quad (9)$$

where n_Φ is the flux per unit cell. The FQAH Jain sequence includes the observed state at filling $\frac{2}{3}$ in $t\text{MoTe}_2$, which has also been studied numerically [8, 9]. In Fig. 2 we present ED evidence for additional Jain FQAH states in $t\text{MoTe}_2$ at $n = \frac{2}{5}$ and its particle-hole conjugate at $n = \frac{3}{5}$.

Intrinsic commensurability oscillations at zero field.

We now explore the host of phenomena arising from an interplay of flux attachment with the presence of the moiré superlattice potential. Indeed, due to the periodic modulation intrinsic to moiré materials, we find that both commensurability oscillations [73–77] and Hofstadter subgaps can be accessed by tuning density *alone*.

Commensurability oscillations occur when the cyclotron radius and the modulation period are commensurate. More precisely, magnetoresistance minima and compressibility maxima are expected when a system in a spatially modulated potential with wave vector Q satisfies the electronic flat band conditions,

$$2k_F Q \ell^2 = 2\pi(j + \phi), \quad (10)$$

where j is a positive integer, ℓ is the effective magnetic length felt by the electric charges, and ϕ is a phase shift. This condition is derived in the Supplemental Material from both perturbative and semiclassical approaches.

Again focusing on the $n = \frac{1}{2}$ ACFL, if the system is doped from half-filling by density, $\delta\rho_e = \rho_e - \bar{\rho}$, the composite fermions feel a magnetic field $b_* = 4\pi\delta\rho_e$ by the flux attachment constraint in Eq. (4). As in the HLR approach, the composite Fermi wave vector of the ACFL described by Eq. (3) is set by the electric charge density, $k_F = \sqrt{4\pi\bar{\rho}}$. We then find that commensurability oscillations occur at densities

$$\delta\rho_e = \frac{k_F Q}{(2\pi)^2} \frac{1}{j + \phi} \quad (11)$$

at large j where $\delta\rho_e$ is small compared to $\bar{\rho}$. For the $n = 1/2$ ACFL, we have $k_F Q = (4\pi^{3/2}/\sqrt{43})/A$ (A is the moiré unit cell area) so that the oscillations correspond to filling frac-

tions, $n = \frac{1}{2} + \delta n$, where

$$\delta n = \frac{1}{\sqrt[3]{3}\sqrt{\pi}} \frac{1}{j + \phi} \approx \frac{0.43}{j + \phi}. \quad (12)$$

Close to $n = 1/2$, the oscillations therefore have period $\Delta(1/\delta n) \approx 2.3$.

We emphasize that in the ACFL these commensurability oscillations occur *in the absence of any external magnetic field*. They coexist with SdH oscillations coming from filling integer Landau levels of composite fermions, which realize Jain states in a clean system. Additionally, tuning density and external field together allows full access of the magnetic spectrum of composite fermions near half-filling of the Chern band.

Discussion. Starting from a band-projected continuum model for $t\text{MoTe}_2$, we have presented exact diagonalization evidence for compressible, non-Fermi liquid states at zero magnetic field, which we dub the anomalous composite Fermi liquid. Much as in conventional fractional quantum Hall systems, we argue that the ACFL picture offers a powerful organizing perspective for understanding fractional quantum anomalous Hall states. Indeed, all of the states for which there currently exists theoretical or experimental evidence fall on the celebrated Jain sequence. We furthermore developed an effective theory capturing the universal properties of the ACFL offering concrete, observable signatures, including commensurability oscillations and Jain sequence FQAH states themselves.

Interestingly, in the recent experiment on $t\text{MoTe}_2$ [1], the coercive field is found to be enhanced at $n = \frac{3}{4}$, in addition to $n = \frac{2}{3}$. Unlike the $n = \frac{2}{3}$ state, which is incompressible, the $n = \frac{3}{4}$ state appears to be compressible. Our theory offers a potential explanation of the observed $n = \frac{3}{4}$ state as the ACFL.

Finally, the emergence of an ACFL state suggests the possibility of new quantum phase transitions not possible at finite field. For example, while our analysis here focuses on zero displacement field, it should be possible to induce a phase transition between ACFL and ferromagnetic Fermi liquid phases by tuning displacement field. Continuous transitions between CFLs and Fermi liquids have been proposed in the past [27, 28]. We leave study of such phase transitions to future work.

Note added. Recently, an independent work by Dong *et al.* [78] appeared, which has some overlapping conclusions with the present study.

Acknowledgements. We are grateful to Xiaodong Xu and Ady Stern for interesting discussions. HG also thanks Jennifer Cano, Mike Mulligan, Sri Raghu, T. Senthil, Raman Sohal, Alex Thomson, and Cenke Xu for conversations on related topics. This work was supported by the Air Force Office of Scientific Research (AFOSR) under award FA9550-22-1-0432 and the David and Lucile Packard Foundation. HG is supported by the Gordon and Betty Moore Foundation EPiQS Initiative through Grant No. GBMF8684 at the Massachusetts Institute of Technology. The authors acknowledge the MIT

SuperCloud and Lincoln Laboratory Supercomputing Center for providing HPC resources that have contributed to the research results reported within this paper.

-
- [1] J. Cai, E. Anderson, C. Wang, X. Zhang, X. Liu, W. Holtzmann, Y. Zhang, F. Fan, T. Taniguchi, K. Watanabe, Y. Ran, T. Cao, L. Fu, D. Xiao, W. Yao, and X. Xu, Signatures of Fractional Quantum Anomalous Hall States in Twisted MoTe_2 , *Nature* [10.1038/s41586-023-06289-w](https://doi.org/10.1038/s41586-023-06289-w) (2023).
 - [2] Y. Zeng, Z. Xia, K. Kang, J. Zhu, P. Knüppel, C. Vaswani, K. Watanabe, T. Taniguchi, K. F. Mak, and J. Shan, Integer and fractional Chern insulators in twisted bilayer MoTe_2 (2023), [arXiv:2305.00973 \[cond-mat.mes-hall\]](https://arxiv.org/abs/2305.00973).
 - [3] F. Wu, T. Lovorn, E. Tutuc, I. Martin, and A. H. MacDonald, Topological Insulators in Twisted Transition Metal Dichalcogenide Homobilayers, *Phys. Rev. Lett.* **122**, 086402 (2019).
 - [4] T. Devakul, V. Crépel, Y. Zhang, and L. Fu, Magic in twisted transition metal dichalcogenide bilayers, *Nature Communications* **12**, 6730 (2021).
 - [5] H. Li, U. Kumar, K. Sun, and S.-Z. Lin, Spontaneous fractional chern insulators in transition metal dichalcogenide moiré superlattices, *Phys. Rev. Res.* **3**, L032070 (2021).
 - [6] V. Crépel and L. Fu, Anomalous hall metal and fractional chern insulator in twisted transition metal dichalcogenides, *Phys. Rev. B* **107**, L201109 (2023).
 - [7] N. Morales-Durán, J. Wang, G. R. Schleder, M. Angeli, Z. Zhu, E. Kaxiras, C. Repellin, and J. Cano, Pressure-enhanced fractional chern insulators in moiré transition metal dichalcogenides along a magic line (2023), [arXiv:2304.06669 \[cond-mat.str-el\]](https://arxiv.org/abs/2304.06669).
 - [8] A. P. Reddy, F. F. Alsallom, Y. Zhang, T. Devakul, and L. Fu, Fractional quantum anomalous Hall states in twisted bilayer MoTe_2 and WSe_2 (2023), [arXiv:2304.12261 \[cond-mat.mes-hall\]](https://arxiv.org/abs/2304.12261).
 - [9] C. Wang, X.-W. Zhang, X. Liu, Y. He, X. Xu, Y. Ran, T. Cao, and D. Xiao, Fractional chern insulator in twisted bilayer mote_2 (2023), [arXiv:2304.11864 \[cond-mat.str-el\]](https://arxiv.org/abs/2304.11864).
 - [10] C. Repellin and T. Senthil, Chern bands of twisted bilayer graphene: Fractional chern insulators and spin phase transition, *Phys. Rev. Res.* **2**, 023238 (2020).
 - [11] A. Abouelkomsan, Z. Liu, and E. J. Bergholtz, Particle-hole duality, emergent fermi liquids, and fractional chern insulators in moiré flatbands, *Phys. Rev. Lett.* **124**, 106803 (2020).
 - [12] P. J. Ledwith, G. Tarnopolsky, E. Khalaf, and A. Vishwanath, Fractional chern insulator states in twisted bilayer graphene: An analytical approach, *Phys. Rev. Res.* **2**, 023237 (2020).
 - [13] Z. Liu, A. Abouelkomsan, and E. J. Bergholtz, Gate-tunable fractional chern insulators in twisted double bilayer graphene, *Phys. Rev. Lett.* **126**, 026801 (2021).
 - [14] J. Wang, J. Cano, A. J. Millis, Z. Liu, and B. Yang, Exact landau level description of geometry and interaction in a flatband, *Phys. Rev. Lett.* **127**, 246403 (2021).
 - [15] D. Parker, P. Ledwith, E. Khalaf, T. Soejima, J. Hauschild, Y. Xie, A. Pierce, M. P. Zaletel, A. Yacoby, and A. Vishwanath, Field-tuned and zero-field fractional chern insulators in magic angle graphene (2021), [arXiv:2112.13837 \[cond-mat.str-el\]](https://arxiv.org/abs/2112.13837).
 - [16] T. Neupert, L. Santos, C. Chamon, and C. Mudry, Fractional quantum hall states at zero magnetic field, *Phys. Rev. Lett.* **106**, 236804 (2011).
 - [17] D. N. Sheng, Z.-C. Gu, K. Sun, and L. Sheng, Fractional quan-

- tum hall effect in the absence of landau levels, *Nature Communications* **2**, 389 (2011).
- [18] N. Regnault and B. A. Bernevig, Fractional chern insulator, *Phys. Rev. X* **1**, 021014 (2011).
- [19] S. Kourtis and M. Daghofer, Combined topological and landau order from strong correlations in chern bands, *Phys. Rev. Lett.* **113**, 216404 (2014).
- [20] S. Kourtis, Symmetry breaking and the fermionic fractional chern insulator in topologically trivial bands, *Phys. Rev. B* **97**, 085108 (2018).
- [21] R. Sohal and E. Fradkin, Intertwined order in fractional chern insulators from finite-momentum pairing of composite fermions, *Phys. Rev. B* **101**, 245154 (2020).
- [22] E. C. Regan, D. Wang, C. Jin, M. I. Bakti Utama, B. Gao, X. Wei, S. Zhao, W. Zhao, Z. Zhang, K. Yumigeta, M. Blei, J. D. Carlström, K. Watanabe, T. Taniguchi, S. Tongay, M. Crommie, A. Zettl, and F. Wang, Mott and generalized Wigner crystal states in WSe₂/WS₂ moirésuperlattices, *Nature* **579**, 359 (2020).
- [23] Y. Xu, S. Liu, D. A. Rhodes, K. Watanabe, T. Taniguchi, J. Hone, V. Elser, K. F. Mak, and J. Shan, Correlated insulating states at fractional fillings of moirésuperlattices, *Nature* **587**, 214 (2020).
- [24] H. Li, S. Li, E. C. Regan, D. Wang, W. Zhao, S. Kahn, K. Yumigeta, M. Blei, T. Taniguchi, K. Watanabe, S. Tongay, A. Zettl, M. F. Crommie, and F. Wang, Imaging two-dimensional generalized wigner crystals, *Nature* **597**, 650 (2021).
- [25] J. Dong, J. Wang, and L. Fu, Dirac electron under periodic magnetic field: Platform for fractional Chern insulator and generalized Wigner crystal, *arXiv e-prints*, [arXiv:2208.10516](https://arxiv.org/abs/2208.10516) (2022), [arXiv:2208.10516 \[cond-mat.mes-hall\]](https://arxiv.org/abs/2208.10516).
- [26] M. Barkeshli and J. McGreevy, Continuous transition between fractional quantum Hall and superfluid states, *Phys. Rev. B* **89**, 235116 (2014), [arXiv:1201.4393 \[cond-mat.str-el\]](https://arxiv.org/abs/1201.4393).
- [27] M. Barkeshli and J. McGreevy, Continuous transitions between composite fermi liquid and landau fermi liquid: A route to fractionalized mott insulators, *Phys. Rev. B* **86**, 075136 (2012).
- [28] L. Zou and D. Chowdhury, Deconfined metal-insulator transitions in quantum hall bilayers, *Phys. Rev. Res.* **2**, 032071 (2020).
- [29] X.-Y. Song, H. Goldman, and L. Fu, Emergent qed₃ from half-filled flat chern bands (2023), [arXiv:2302.10169 \[cond-mat.str-el\]](https://arxiv.org/abs/2302.10169).
- [30] B. I. Halperin, P. A. Lee, and N. Read, Theory of the half filled Landau level, *Phys. Rev. B* **47**, 7312 (1993).
- [31] B. I. Halperin, The Half-Full Landau Level, in *Fractional Quantum Hall Effects: New Developments* (World Scientific, 2020) pp. 79–132.
- [32] J. K. Jain, Composite-fermion approach for the fractional quantum Hall effect, *Phys. Rev. Lett.* **63**, 199 (1989).
- [33] A. López and E. Fradkin, Fractional quantum Hall effect and Chern-Simons gauge theories, *Phys. Rev. B* **44**, 5246 (1991).
- [34] S. Kivelson, D.-H. Lee, and S.-C. Zhang, Global phase diagram in the quantum hall effect, *Phys. Rev. B* **46**, 2223 (1992).
- [35] J. H. Smet, K. von Klitzing, D. Weiss, and W. Wegscheider, dc transport of composite fermions in weak periodic potentials, *Phys. Rev. Lett.* **80**, 4538 (1998).
- [36] J. H. Smet, S. Jobst, K. von Klitzing, D. Weiss, W. Wegscheider, and V. Umansky, Commensurate composite fermions in weak periodic electrostatic potentials: Direct evidence of a periodic effective magnetic field, *Phys. Rev. Lett.* **83**, 2620 (1999).
- [37] R. L. Willett, K. W. West, and L. N. Pfeiffer, Geometric resonance of composite fermion cyclotron orbits with a fictitious magnetic field modulation, *Phys. Rev. Lett.* **83**, 2624 (1999).
- [38] D. Kamburov, M. Shayegan, L. N. Pfeiffer, K. W. West, and K. W. Baldwin, Commensurability oscillations of hole-flux composite fermions, *Phys. Rev. Lett.* **109**, 236401 (2012).
- [39] D. Kamburov, Y. Liu, M. A. Mueed, M. Shayegan, L. N. Pfeiffer, K. W. West, and K. W. Baldwin, What determines the fermi wave vector of composite fermions?, *Phys. Rev. Lett.* **113**, 196801 (2014).
- [40] H. Deng, Y. Liu, I. Jo, L. N. Pfeiffer, K. W. West, K. W. Baldwin, and M. Shayegan, Commensurability oscillations of composite fermions induced by the periodic potential of a wigner crystal, *Phys. Rev. Lett.* **117**, 096601 (2016).
- [41] C. Wang, N. R. Cooper, B. I. Halperin, and A. Stern, Particle-hole symmetry in the fermion-cheren-simons and dirac descriptions of a half-filled landau level, *Phys. Rev. X* **7**, 031029 (2017).
- [42] A. K. C. Cheung, S. Raghu, and M. Mulligan, Weiss oscillations and particle-hole symmetry at the half-filled Landau level, *Phys. Rev. B* **95**, 235424 (2017).
- [43] A. Mitra and M. Mulligan, Fluctuations and magnetoresistance oscillations near the half-filled landau level, *Phys. Rev. B* **100**, 165122 (2019).
- [44] M. Shayegan, Probing composite fermions near half-filled landau levels, in *Fractional Quantum Hall Effects: New Developments* (World Scientific, 2020) pp. 133–181.
- [45] Y.-W. Lu, P. Kumar, and M. Mulligan, Weiss oscillations and galilei invariance (2023), [arXiv:2302.14076 \[cond-mat.str-el\]](https://arxiv.org/abs/2302.14076).
- [46] Y. Saito, F. Yang, J. Ge, X. Liu, T. Taniguchi, K. Watanabe, J. I. A. Li, E. Berg, and A. F. Young, Isospin pomeranchuk effect in twisted bilayer graphene, *Nature* **592**, 220 (2021).
- [47] T. Li, S. Jiang, L. Li, Y. Zhang, K. Kang, J. Zhu, K. Watanabe, T. Taniguchi, D. Chowdhury, L. Fu, J. Shan, and K. F. Mak, Continuous mott transition in semiconductor moirésuperlattices, *Nature* **597**, 350 (2021).
- [48] D. N. Sheng and L. Fu, Thermoelectric response and entropy of fractional quantum hall systems, *Phys. Rev. B* **101**, 241101 (2020).
- [49] F. D. M. Haldane, Many-particle translational symmetries of two-dimensional electrons at rational landau-level filling, *Phys. Rev. Lett.* **55**, 2095 (1985).
- [50] Y.-L. Wu, N. Regnault, and B. A. Bernevig, Bloch model wave functions and pseudopotentials for all fractional chern insulators, *Physical review letters* **110**, 106802 (2013).
- [51] B. A. Bernevig and N. Regnault, Emergent many-body translational symmetries of abelian and non-abelian fractionally filled topological insulators, *Physical Review B* **85**, 075128 (2012).
- [52] J. K. Jain, Incompressible quantum hall states, *Phys. Rev. B* **40**, 8079 (1989).
- [53] X.-G. Wen, Theory of the edge states in fractional quantum Hall effects, *Int. J. Mod. Phys. B* **6**, 1711 (1992).
- [54] A. Vaezi, Fractional quantum hall effect at zero magnetic field (2011), [arXiv:1105.0406 \[cond-mat.str-el\]](https://arxiv.org/abs/1105.0406).
- [55] Y.-M. Lu and Y. Ran, Symmetry-protected fractional chern insulators and fractional topological insulators, *Phys. Rev. B* **85**, 165134 (2012).
- [56] R. Sohal, L. H. Santos, and E. Fradkin, Chern-simons composite fermion theory of fractional chern insulators, *Phys. Rev. B* **97**, 125131 (2018).
- [57] A. H. MacDonald, Landau-level subband structure of electrons on a square lattice, *Phys. Rev. B* **28**, 6713 (1983).
- [58] Y.-M. Lu, Y. Ran, and M. Oshikawa, Filling-enforced constraint on the quantized hall conductivity on a periodic lattice, *Annals of Physics* **413**, 168060 (2020).
- [59] N. Manjunath and M. Barkeshli, Crystalline gauge fields and quantized discrete geometric response for abelian topological

- phases with lattice symmetry, *Phys. Rev. Res.* **3**, 013040 (2021).
- [60] A. B. Pippard, Quantization of coupled orbits in metals, *Proc. R. Soc. London A - Math. Phys. Sci.* **270**, 1 (1962).
- [61] A. B. Pippard, Quantization of coupled orbits in metals II. The two-dimensional network, with special reference to the properties of zinc, *Philosophical Transactions of the Royal Society of London. Series A, Mathematical and Physical Sciences* **256**, 317 (1964).
- [62] S. M. Girvin, Particle-hole symmetry in the anomalous quantum hall effect, *Phys. Rev. B* **29**, 6012 (1984).
- [63] D. T. Son, Is the composite fermion a dirac particle?, *Phys. Rev. X* **5**, 031027 (2015).
- [64] H. Goldman and E. Fradkin, Dirac Composite Fermions and Emergent Reflection Symmetry about Even Denominator Filling Fractions, *Phys. Rev. B* **98**, 165137 (2018), [arXiv:1808.09314 \[cond-mat.str-el\]](https://arxiv.org/abs/1808.09314).
- [65] P. Kumar, M. Mulligan, and S. Raghu, Topological phase transition underpinning particle-hole symmetry in the Halperin-Lee-Read theory, *Phys. Rev. B* **98**, 115105 (2018), [arXiv:1805.06462 \[cond-mat.str-el\]](https://arxiv.org/abs/1805.06462).
- [66] P. Kumar, M. Mulligan, and S. Raghu, Emergent reflection symmetry from nonrelativistic composite fermions, *Phys. Rev. B* **99**, 205151 (2019).
- [67] Z. Dong and T. Senthil, Noncommutative field theory and composite Fermi liquids in some quantum Hall systems, *Phys. Rev. B* **102**, 205126 (2020), [arXiv:2006.01282 \[cond-mat.str-el\]](https://arxiv.org/abs/2006.01282).
- [68] Z. Dong and T. Senthil, Evolution between quantum hall and conducting phases: Simple models and some results, *Phys. Rev. B* **105**, 085301 (2022).
- [69] H. Goldman and T. Senthil, Lowest landau level theory of the bosonic jain states, *Phys. Rev. B* **105**, 075130 (2022).
- [70] S. Predin, A. Knezević, and M. Milovanović, Dipole representation of half-filled landau level, *Physical Review B* **107**, 155132 (2023).
- [71] G. Möller and N. R. Cooper, Composite fermion theory for bosonic quantum hall states on lattices, *Phys. Rev. Lett.* **103**, 105303 (2009).
- [72] E. Tang, J.-W. Mei, and X.-G. Wen, High-temperature fractional quantum hall states, *Phys. Rev. Lett.* **106**, 236802 (2011).
- [73] D. Weiss, K. V. Klitzing, K. Ploog, and G. Weimann, Magnetoresistance Oscillations in a Two-Dimensional Electron Gas Induced by a Submicrometer Periodic Potential, *Europhys. Lett.* **8**, 179 (1989).
- [74] R. R. Gerhardts, D. Weiss, and K. v. Klitzing, Novel magnetoresistance oscillations in a periodically modulated two-dimensional electron gas, *Phys. Rev. Lett.* **62**, 1173 (1989).
- [75] R. W. Winkler, J. P. Kotthaus, and K. Ploog, Landau band conductivity in a two-dimensional electron system modulated by an artificial one-dimensional superlattice potential, *Phys. Rev. Lett.* **62**, 1177 (1989).
- [76] D. Weiss, Magnetoquantum oscillations in a lateral superlattice, in *Electronic Properties of Multilayers and Low-Dimensional Semiconductor Structures*, edited by J. M. Chamberlain, L. Eaves, and J.-C. Portal (Springer US, Boston, MA, 1990) pp. 133–150.
- [77] R. R. Gerhardts, Quasiclassical calculation of magnetoresistance oscillations of a two-dimensional electron gas in spatially periodic magnetic and electrostatic fields, *Phys. Rev. B* **53**, 11064 (1996).
- [78] J. Dong, J. Wang, P. J. Ledwith, A. Vishwanath, and D. E. Parker, Composite fermi liquid at zero magnetic field in twisted mote₂ (2023), [arXiv:2306.01719 \[cond-mat.str-el\]](https://arxiv.org/abs/2306.01719).

Supplemental material: Zero-field composite Fermi liquid in twisted semiconductor bilayers

Hart Goldman, Aidan P. Reddy, Nisarga Paul, and Liang Fu
Department of Physics, Massachusetts Institute of Technology, Cambridge, MA 02139

EXACT DIAGONALIZATION METHODOLOGY AND EXTENDED DATA

Our exact diagonalization calculation starts with the single-particle continuum model for AA-stacked, K-valley TMD moiré homobilayers:

$$H_0 = \sum_{\sigma=\uparrow,\downarrow} \int d\mathbf{r} \psi_{\sigma}^{\dagger}(\mathbf{r}) \mathcal{H}_{\sigma} \psi_{\sigma}(\mathbf{r}). \quad (1)$$

Here \mathcal{H}_{σ} is a 2×2 matrix in layer pseudospin,

$$\mathcal{H}_{\uparrow} = \begin{pmatrix} \frac{\hbar^2(-i\nabla-\kappa_{+})^2}{2m} + V_1(\mathbf{r}) & t(\mathbf{r}) \\ t^{\dagger}(\mathbf{r}) & \frac{\hbar^2(-i\nabla-\kappa_{-})^2}{2m} + V_2(\mathbf{r}) \end{pmatrix} \quad (2)$$

where

$$V_i(\mathbf{r}) = -2V \sum_{i=1,3,5} \cos(\mathbf{g}_i \cdot \mathbf{r} + (-1)^i \phi), \quad (3)$$

$$t(\mathbf{r}) = w(1 + e^{i\mathbf{g}_2 \cdot \mathbf{r}} + e^{i\mathbf{g}_3 \cdot \mathbf{r}}), \quad (4)$$

and $\mathbf{g}_i = \frac{4\pi}{\sqrt{3}a_M} (\cos \frac{\pi(i-1)}{3}, \sin \frac{\pi(i-1)}{3})$, $\kappa_{-} = \frac{\mathbf{g}_1 + \mathbf{g}_6}{3}$, $\kappa_{+} = \frac{\mathbf{g}_1 + \mathbf{g}_2}{3}$. \mathcal{H}_{\downarrow} is fixed by \mathcal{H}_{\uparrow} and the time-reversal symmetry condition $\mathcal{T}H_0\mathcal{T}^{-1} = H_0$. Due to large spin-orbit splitting at the monolayer valence band maxima, the spin and valley are locked at low energies into a single ‘‘spin’’ quantum number indexed by σ . This model has been derived and its rich single-particle properties discussed elsewhere [1–3]. We work under a particle-hole transformation $c_{\mathbf{k}\uparrow} \rightarrow c_{\mathbf{k}\uparrow}^{\dagger}$ so that the spectrum is bounded from below.

We study the model’s many-body physics by adding a Coulomb interaction $V(r) = \frac{e^2}{\epsilon r}$ and projecting to the lowest moiré band, yielding the projected Hamiltonian

$$\tilde{H} = \sum_{\mathbf{k},\sigma} \varepsilon_{\mathbf{k}\sigma} c_{\mathbf{k}\sigma}^{\dagger} c_{\mathbf{k}\sigma} + \frac{1}{2} \sum_{\mathbf{k}'\mathbf{p}'\mathbf{k}\mathbf{p},\sigma\sigma'} V_{\mathbf{k}'\mathbf{p}'\mathbf{k}\mathbf{p};\sigma\sigma'} c_{\mathbf{k}'\sigma}^{\dagger} c_{\mathbf{p}'\sigma'}^{\dagger} c_{\mathbf{p}\sigma'} c_{\mathbf{k}\sigma} \quad (5)$$

where $c_{\mathbf{k}\sigma}^{\dagger}$ creates a hole with moiré crystal momentum \mathbf{k} spin/valley quantum number σ with band energy $\varepsilon_{\mathbf{k}\sigma}$. $V_{\mathbf{k}'\mathbf{p}'\mathbf{k}\mathbf{p};\sigma\sigma'} \equiv \langle \mathbf{k}'\sigma'; \mathbf{p}'\sigma' | \hat{V} | \mathbf{k}\sigma; \mathbf{p}\sigma' \rangle$ are the Bloch state interaction matrix elements. This method can be viewed as a variational approximation of the ground and low-lying excited states with the Fock space of the lowest moiré band as the variational Hilbert subspace. This variational approximation is designed to be exact in the absence of interactions and will be generically inexact in their presence.

The torus geometries used in the exact diagonalization calculations shown in this work are defined by the boundary condition wavevectors $\mathbf{L}_1, \mathbf{L}_2$. The 16-unit-cell cluster is defined by $\mathbf{L}_i^{(16)} = 4\mathbf{a}_i$ and the 30-unit-cell cluster by $\mathbf{L}_1^{(30)} = 5\mathbf{a}_1, \mathbf{L}_2^{(30)} = 6\mathbf{a}_2$ where $\mathbf{a}_1 = \lambda(\frac{1}{2}, \frac{\sqrt{3}}{2})$, $\mathbf{a}_2 = \lambda(0, 1)$. $\lambda = a_M$ in the case of the moiré system and $\lambda = \frac{\sqrt{2\pi\ell^2}}{\sqrt{3}/2}$ in the case of the LLL where ℓ is the magnetic length such that the moiré and magnetic unit cells correspond.

In the moiré case, the many-body crystal momentum quantum number \mathbf{k} of a given many-body state $|\Psi\rangle$ is defined as $\mathbf{T}_{\mathbf{a}_i}^{CM} |\Psi\rangle = e^{i\mathbf{k}\cdot\mathbf{a}_i} |\Psi\rangle$ where $\mathbf{T}_{\mathbf{d}}^{CM} = \prod_i e^{i\mathbf{p}_i \cdot \mathbf{d}}$ is an ordinary center-of-mass translation operator where the index i labels particles. $\mathbf{k} = k_1\mathbf{T}_1 + k_2\mathbf{T}_2$ where $\mathbf{L}_i = N_i\mathbf{a}_i$, and $\mathbf{T}_1 = \frac{2\pi\epsilon_{ij}\mathbf{L}_j \times \hat{z}}{|\mathbf{L}_1 \times \mathbf{L}_2|}$. In the case of the LLL, we define the many-body crystal momentum quantum number as the eigenvalue under a center-of-mass *magnetic* translation by a primitive lattice vector $t_{\mathbf{a}_i}^{CM} |\Psi\rangle = e^{i\mathbf{k}\cdot\mathbf{a}_i} |\Psi\rangle$ where $t_{\mathbf{d}}^{CM} = \prod_i t_{\mathbf{d}}^i$ is the center-of-mass magnetic translation operator. Ref. [4] explains how to construct set of the LLL single-particle states on a torus that transform like Bloch states under *magnetic* translations,

$t_{\mathbf{a}_i} |\psi_{\mathbf{k}}\rangle = e^{i\mathbf{k}\cdot\mathbf{a}_i} |\psi_{\mathbf{k}}\rangle$. A Fock state constructed from a set of these single-particle states has center-of-mass magnetic crystal momentum equal to the sum of the magnetic crystal momenta of those single-particle states, analogously to the zero- B moiré case. We note that this approach does not exploit the full many-body translation symmetries present in a Landau level (originally presented in Ref. [5] and explained more pedagogically in Ref. [6]), but is convenient in this case because it allows for direct comparison with the moiré system.

We use the continuum model parameters reported in Ref. [3] for $t\text{MoTe}_2$. A more detailed account of our continuum model exact diagonalization methods is presented in the Supplemental Material of Ref. [3].

In Fig. 1, we provide evidence that the same qualitative results for the composite Fermi liquid and ferromagnetic metal at $n = \frac{1}{2}$ occur in the presence of weaker Coulomb interaction $\epsilon = 20$. In Fig 2(a), we show the ED spectrum of the LLL at $\nu = \frac{3}{4}$ with which Fig. 1(c) can be compared. Finally, in Fig. 2(b), we show that the spectrum of the moiré AFCL at $n = \frac{3}{4}$, $\theta = 1.9^\circ$ resembles its LLL cousin even more closely than at $\theta = 2^\circ$ shown in Fig 1(c) of the main text.

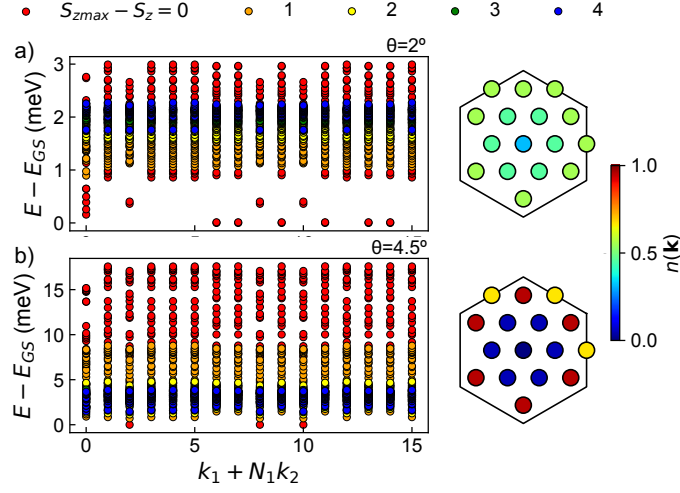


FIG. 1. **Robustness of AFCL and ferromagnetic metal against weaker interaction.** Analogous data to that shown in Fig. 1 of the main text at $n = \frac{1}{2}$ but in the presence of a weaker Coulomb interaction $\epsilon = 20$.

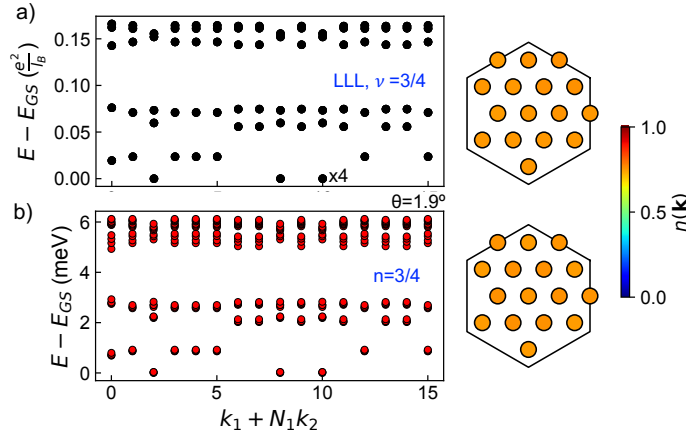


FIG. 2. **ACFL at $n = \frac{3}{4}$** (a) Spectrum of fully spin-polarized electrons with a Coulomb interaction at $\nu = \frac{3}{4}$ in the LLL. Its low-lying states have the same many-body momenta and degeneracy as in the lowest moiré band shown in Fig. 1(c) of the main text. (b) Corresponding spectrum in the lowest moiré band at $\theta = 1.9^\circ$, $\epsilon = 10$, resembling the LLL even more closely than $\theta = 2^\circ$ shown in Fig. 1(c) of the main text. On the right hand side are the occupation numbers of the single-particle crystal momentum states averaged over the 12-fold nearly degenerate ground state manifold, demonstrating the absence of an electronic Fermi surface. The lowest 20 energy levels in each momentum sector are shown.

PARTON CONSTRUCTION OF THE ACFL EFFECTIVE THEORY

Despite the absence of external magnetic flux in the Chern band context, much of the physics of flux attachment persists if we adopt a perspective where the physical electrons, denoted c , are fractionalized into emergent parton degrees of freedom,

$$c_x = \phi_x \psi_x. \quad (6)$$

Here ϕ is taken to be a bosonic “holon” that carries the physical electric charge, while ψ is a neutral fermionic “spinon.” Using this parton description allows for a simple extension of the intuition of flux attachment to the Chern band setting [7–13]. However, we note recent efforts to construct lattice flux attachment procedures for constructing FQAH and fractional Chern insulator phases [14, 15].

The above parton decomposition has a local gauge redundancy, under which $\psi_x \rightarrow e^{i\theta_x} \psi_x$ and $\phi_x \rightarrow e^{-i\theta_x} \phi_x$, meaning that both must also couple to an emergent U(1) gauge field which we denote $a_\mu = (a_t, a_x, a_y)$. In summary, ϕ couples to the combination $A_\mu - a_\mu$, where $A_\mu = (A_t, A_x, A_y)$ is the physical (background) electromagnetic gauge field, while ψ couples to a_μ alone. We will assume that the system is in a regime where gauge fluctuations do not confine the partons.

Previously, Refs. [13, 16] applied the parton decomposition in Eq. 6 to study ACFL phases starting from lattice tight binding models. Here, with an eye toward moiré systems, we approach the emergence of the ACFL from a more long wavelength perspective. We treat the long-wavelength moiré superlattice as a periodic electric scalar potential, $A_t = \mathcal{V}(x)$. Then, neglecting gauge fluctuations, $\langle a_\mu \rangle = 0$, the holons, ϕ , will see the same band structure as the electrons in the physical system of interest.

Considering the example of $t\text{MoTe}_2$, at sufficient twist angle time-reversal symmetry is broken due to spontaneous Ising ferromagnetism, and a narrow $C = -1$ flat band occurs. If the physical electrons fill half fill this band, then so too do the holons (at mean field level), since they see the same superlattice potential. Because the holons are bosons, they then form an incompressible, *bosonic FQAH state* with the same topological order as the $\nu = -1/2$ bosonic Laughlin state and Hall conductivity, $\sigma_{xy}^\phi = -e^2/2h$. They may be integrated out to yield the FQAH topological quantum field theory (TQFT) [17–19],

$$\mathcal{L}_\phi = \frac{2}{4\pi} bdb + \frac{1}{2\pi} bd(A - a) + (A_t - a_t) \bar{\rho}, \quad (7)$$

where we have introduced an auxiliary gauge field, b_μ . We define $\bar{\rho}$ to be the value of the physical charge density, such that the filling is $\bar{\rho} \times (\text{moiré unit cell area}) \equiv \mathfrak{s} = +1/2$. Indeed, the main difference with the usual continuum bosonic Laughlin TQFT is the presence of the final term, which gives the charge “glued” to the superlattice and guarantees that the theory makes sense in the absence of an external magnetic field. Notably, in a FQAH or fractional Chern insulator (FCI) state at finite field, $\mathfrak{s}n \in \mathbb{Z}$ should be quantized in units of the topological degeneracy on the torus, n [18].

Assuming that at long wavelengths the spinons can be described with a quadratic dispersion and effective mass, m_* , one then obtains a final effective theory for the Chern band system at half-filling,

$$\begin{aligned} \mathcal{L}_{\text{ACFL}} = & \psi^\dagger (i\partial_t + a_t) \psi - \frac{1}{2m_*} |(i\partial_i + a_i)\psi|^2 \\ & + \frac{2}{4\pi} bdb + \frac{1}{2\pi} bd(A - a) + (A_t - a_t) \bar{\rho}. \end{aligned} \quad (8)$$

Integrating out b_μ and shifting $a \rightarrow a + A$ gives the effective Lagrangian in Eq. (3) of the main text. However, only the Lagrangian with b_μ included is gauge invariant on arbitrary manifolds.

We remark that the procedure outlined here holds whether or not the holon FQAH state is chosen to have nontrivial spatial symmetry fractionalization. Indeed, we conjecture that an advantage of the composite fermion framework is that the choice of symmetry fractionalization pattern for the holon FQAH state *determines* the symmetry fractionalization of the Jain sequence states built up by filling Landau levels of composite fermions. We plan to present a more detailed discussion of the composite fermion point of view for spatial symmetry enrichment in future work.

COMMENSURABILITY OSCILLATIONS

A distinguishing feature of the anomalous composite Fermi liquid (ACFL) is that it will display commensurability oscillations as a function of density alone due to its in-built moiré periodic potential, while an ordinary Fermi liquid or finite-field CFL will not. In contrast, GaAs displays commensurability oscillations due to an *externally* applied periodical scalar or vector potential [20] and at finite field. Upon doping away from half-filling, $\bar{\rho} = \frac{1}{2} A_{\text{u.c.}}^{-1}$, the composite fermions feel an effective magnetic field $b_* = 4\pi(\rho_e - \bar{\rho})$. Let us assume that the added density (and thus b_*) is spatially uniform. We can treat this system

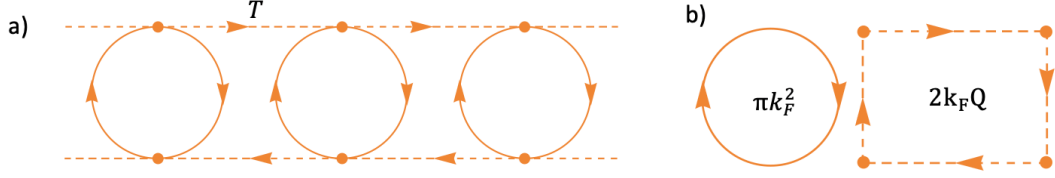


FIG. 3. **Network model.** (a) Network model capturing commensurability oscillations due to tunneling T between Fermi surfaces in repeated zone scheme. (b) Relevant k -space orbits and areas.

as a parabolic band of fermions with effective mass m^* in a magnetic field b_* and a periodic scalar potential. The potential has triangular lattice symmetry with wavevector Q and strength V_0 . The composite fermions half-fill the lowest band of the moiré Brillouin zone.

In this section we discuss the perturbative and semiclassical approaches to commensurability oscillations. While the former approach is well known, discussions of the latter approach are lacking. The advantage of the latter is that it shows that commensurability oscillations naturally arise even in a nonperturbative regime $V_0 \gg \omega_c$; indeed, the ACFL may be in this regime at small b_* .

Perturbative approach. As noted in Ref. [21], magnetoresistance minima occur at the electron flat band condition. To first order in perturbation theory, the bandwidth of the n 'th Landau level in a scalar potential of wavevector Q is controlled by the factor

$$e^{-Q^2 \ell^2 / 4} L_n(Q^2 \ell^2 / 2) = \frac{\cos(\sqrt{2n} Q \ell - \frac{\pi}{4})}{\sqrt{\pi Q \ell} \sqrt{n/2}} + O(n^{-3/4}) \quad (9)$$

so at large n , using the fact that $n = \rho_e 2\pi \ell^2$ and $k_F = \sqrt{4\pi \rho_e}$, we have the flat band condition $2k_F Q \ell^2 = 2\pi(j - 1/4)$. This implies $2R_c/a = j - 1/4$ when $a = 2\pi/Q$, while for the triangular lattice this implies $4R_c/\sqrt{3}a = j - 1/4$ [22]. For composite fermions, this condition becomes $2\sqrt{4\pi(\bar{\rho} + \Delta\rho_e)}Q/4\pi\Delta\rho_e = 2\pi(j - 1/4)$, which yields Eq. (11) of the main text at large j .

Semiclassical approach. We follow the semiclassical network model approach to the magnetic density of states as in [23–25]. Consider the network model shown in Fig. 3. For simplicity we are considering a 1D modulation instead of a 2D modulation, since the nature of commensurability oscillations doesn't change qualitatively between the two. We are assuming some phenomenological tunneling T between Fermi surfaces in neighboring zones. The tunneling is best thought of as wavepacket tunneling over a barrier (in k -space). The barrier is set by the dispersion, and hence T depends on V_0 . Although it can occur at other points in the Fermi surface, the tunneling is peaked when the velocity is normal to the barrier; hence as a simplified model we have taken a single hopping between Fermi surface tops and bottoms.

To describe scattering at the junctions, we adopt a basis where $(0, 1)^T$ and $(1, 0)^T$ are the dashed and straight incoming edges, respectively. After a suitable gauge transformation, the scattering unitary at the junction can be written as

$$U = \begin{pmatrix} \sqrt{1-T^2} e^{2\pi i \phi} & -T \\ T & \sqrt{1-T^2} e^{-2\pi i \phi} \end{pmatrix}. \quad (10)$$

Together with the requirement that electrons pick up phases along links so that the total phase around any closed orbit is equal to the corresponding Aharonov-Bohm flux, this specifies the network model completely. We solve for the spectrum at a given magnetic field B by solving for eigenmodes. Valid eigenmodes must be periodic (up to phase) in the repeated Brillouin zone.

Let $S_0 = \pi k_F^2$ and $S_\square = 2k_F Q$. Note S_\square is not the area of any valid closed orbit, but $S_1 = S_0 + S_\square$ is. Next, note that the network could be considered as 1D array of area- S_1 closed orbits, whose mutual overlaps are the area- S_0 orbits. These correspond to the “original” and “lens” orbits of Ref. [25]. It follows from the analysis of Ref. [25] that there is a *flat band* whenever S_0 and S_1 are both quantized, or, equivalently, whenever S_0 and S_\square are both quantized. (A flat band in the network model corresponds to an extensive set of localized eigenmodes). In short, flat bands occur when

$$\ell^2 S_0 = 2\pi(n + \gamma) \quad (11)$$

$$\ell^2 S_\square = 2\pi(m - \phi) \quad (12)$$

where m, n are suitable integers and $\gamma = \frac{1}{2}$ is a Maslov correction. Using $k_F^2 = 2mE$, Eq. 11 is $E = \omega_c(n + 1/2)$ while Eq. 12 is precisely the commensurability condition $2k_F Q \ell^2 = 2\pi(j - \phi)$ for $\phi = 1/4$. The flat band condition coincides with a compressibility maximum and resistance minimum. Note that the all-orders in V_0/ω_c dependence is encoded in T , which does

not affect the final result. The agreement of the two approaches supports the robustness of the commensurability oscillations across the relevant range of b_* .

COMMENT ON PH SYMMETRY AND THE POSSIBILITY OF A DIRAC COMPOSITE FERMION

We wish to remark here on the possibility of particle-hole (PH) symmetry in the ACFL. While PH is present microscopically in the LLL [26] – leading to proposals of Dirac CFLs [27, 28] with an emergent π Fermi surface Berry phase – the Chern band systems we study lack PH symmetry [3], and we anticipate PH asymmetry to occur between states at Chern band fillings $n < 1/2$ and $n > 1/2$. Nevertheless, it is possible that a PH symmetric response can be an emergent property. In particular, recent work has proposed the emergence of PH and so-called reflection symmetries starting from an HLR description [29–31], for example on including the effect of disorder. We leave this direction to future work.

-
- [1] F. Wu, T. Lovorn, E. Tutuc, I. Martin, and A. H. MacDonald, Topological Insulators in Twisted Transition Metal Dichalcogenide Homobilayers, *Phys. Rev. Lett.* **122**, 086402 (2019).
- [2] T. Devakul, V. Crépel, Y. Zhang, and L. Fu, Magic in twisted transition metal dichalcogenide bilayers, *Nature Communications* **12**, 6730 (2021).
- [3] A. P. Reddy, F. F. Alsallom, Y. Zhang, T. Devakul, and L. Fu, Fractional quantum anomalous Hall states in twisted bilayer MoTe_2 and WSe_2 (2023), [arXiv:2304.12261 \[cond-mat.mes-hall\]](https://arxiv.org/abs/2304.12261).
- [4] Y.-L. Wu, N. Regnault, and B. A. Bernevig, Bloch model wave functions and pseudopotentials for all fractional chern insulators, *Physical review letters* **110**, 106802 (2013).
- [5] F. D. M. Haldane, Many-particle translational symmetries of two-dimensional electrons at rational landau-level filling, *Phys. Rev. Lett.* **55**, 2095 (1985).
- [6] B. A. Bernevig and N. Regnault, Emergent many-body translational symmetries of abelian and non-abelian fractionally filled topological insulators, *Physical Review B* **85**, 075128 (2012).
- [7] J. K. Jain, Incompressible quantum hall states, *Phys. Rev. B* **40**, 8079 (1989).
- [8] X.-G. Wen, Theory of the edge states in fractional quantum Hall effects, *Int. J. Mod. Phys. B* **6**, 1711 (1992).
- [9] A. Vaezi, Fractional quantum hall effect at zero magnetic field (2011), [arXiv:1105.0406 \[cond-mat.str-el\]](https://arxiv.org/abs/1105.0406).
- [10] Y.-M. Lu and Y. Ran, Symmetry-protected fractional chern insulators and fractional topological insulators, *Phys. Rev. B* **85**, 165134 (2012).
- [11] J. McGreevy, B. Swingle, and K.-A. Tran, Wave functions for fractional chern insulators, *Phys. Rev. B* **85**, 125105 (2012).
- [12] M. Barkeshli and J. McGreevy, Continuous transition between fractional quantum Hall and superfluid states, *Phys. Rev. B* **89**, 235116 (2014), [arXiv:1201.4393 \[cond-mat.str-el\]](https://arxiv.org/abs/1201.4393).
- [13] M. Barkeshli and J. McGreevy, Continuous transitions between composite fermi liquid and landau fermi liquid: A route to fractionalized mott insulators, *Phys. Rev. B* **86**, 075136 (2012).
- [14] R. Sohal, L. H. Santos, and E. Fradkin, Chern-simons composite fermion theory of fractional chern insulators, *Phys. Rev. B* **97**, 125131 (2018).
- [15] R. Sohal and E. Fradkin, Intertwined order in fractional chern insulators from finite-momentum pairing of composite fermions, *Phys. Rev. B* **101**, 245154 (2020).
- [16] L. Zou and D. Chowdhury, Deconfined metal-insulator transitions in quantum hall bilayers, *Phys. Rev. Res.* **2**, 032071 (2020).
- [17] A. H. MacDonald, Landau-level subband structure of electrons on a square lattice, *Phys. Rev. B* **28**, 6713 (1983).
- [18] Y.-M. Lu, Y. Ran, and M. Oshikawa, Filling-enforced constraint on the quantized hall conductivity on a periodic lattice, *Annals of Physics* **413**, 168060 (2020).
- [19] N. Manjunath and M. Barkeshli, Crystalline gauge fields and quantized discrete geometric response for abelian topological phases with lattice symmetry, *Phys. Rev. Res.* **3**, 013040 (2021).
- [20] D. Kamburov, Y. Liu, M. A. Mueed, M. Shayegan, L. N. Pfeiffer, K. W. West, and K. W. Baldwin, What determines the fermi wave vector of composite fermions?, *Phys. Rev. Lett.* **113**, 196801 (2014).
- [21] R. R. Gerhardts, Quasiclassical calculation of magnetoresistance oscillations of a two-dimensional electron gas in spatially periodic magnetic and electrostatic fields, *Phys. Rev. B* **53**, 11064 (1996).
- [22] D. Weiss, K. V. Klitzing, K. Ploog, and G. Weimann, Magnetoresistance Oscillations in a Two-Dimensional Electron Gas Induced by a Submicrometer Periodic Potential, *Europhys. Lett.* **8**, 179 (1989).
- [23] A. B. Pippard, Quantization of coupled orbits in metals, *Proc. R. Soc. London A - Math. Phys. Sci.* **270**, 1 (1962).
- [24] A. B. Pippard, Quantization of coupled orbits in metals II. The two-dimensional network, with special reference to the properties of zinc, *Philosophical Transactions of the Royal Society of London. Series A, Mathematical and Physical Sciences* **256**, 317 (1964).
- [25] N. Paul, P. J. D. Crowley, T. Devakul, and L. Fu, Moiré Landau Fans and Magic Zeros, *Phys. Rev. Lett.* **129**, 116804 (2022).
- [26] S. M. Girvin, Particle-hole symmetry in the anomalous quantum hall effect, *Phys. Rev. B* **29**, 6012 (1984).
- [27] D. T. Son, Is the composite fermion a dirac particle?, *Phys. Rev. X* **5**, 031027 (2015).
- [28] H. Goldman and E. Fradkin, Dirac Composite Fermions and Emergent Reflection Symmetry about Even Denominator Filling Fractions, *Phys. Rev. B* **98**, 165137 (2018), [arXiv:1808.09314 \[cond-mat.str-el\]](https://arxiv.org/abs/1808.09314).

- [29] C. Wang, N. R. Cooper, B. I. Halperin, and A. Stern, Particle-hole symmetry in the fermion-chern-simons and dirac descriptions of a half-filled landau level, [Phys. Rev. X **7**, 031029 \(2017\)](#).
- [30] P. Kumar, M. Mulligan, and S. Raghu, Topological phase transition underpinning particle-hole symmetry in the Halperin-Lee-Read theory, [Phys. Rev. B **98**, 115105 \(2018\)](#), [arXiv:1805.06462 \[cond-mat.str-el\]](#).
- [31] P. Kumar, M. Mulligan, and S. Raghu, Emergent reflection symmetry from nonrelativistic composite fermions, [Phys. Rev. B **99**, 205151 \(2019\)](#).